Noncanonical Nf-κB Activation by Icariin-Triggered CEBP-β/G-CSF Axis Confers Neuroprotection in Ischemic Optic Neuropathy

Tushar Dnyaneshwar Desai
Hualien Tzu Chi Hospital
Yao-Tseng Wen
Hualien Tzu Chi Hospital
Jayasimha Daddam Rayalu
Agricultural Research Organization Volcani Center
Rong Kung Tsai (rktsai@tzuchi.com.tw)
Hualien Tzu Chi Hospital https://orcid.org/0000-0001-8760-5739

Research article

Keywords: Non-canonical Nf-κB signaling, CEBP-β, Granulocyte colony-stimulating factor, Neuroprotection , Ischemic neuropathy

Posted Date: May 27th, 2021

DOI: https://doi.org/10.21203/rs.3.rs-517426/v1

Abstract

Background

An ischemic insult at the optic nerve is followed by detrimental neuroinflammation that results in the loss of the retinal ganglion cells (RGCs) and vision. NF-κB is the key transcription factor of inflammatory cytokines in response to neuroinflammatory events. Icariin, an anti-inflammatory drug, is involved in the regulation of NF-κB activation. However, the protective mechanisms of icariin-induced NF-κB activation remain little known. Here, the protective mechanisms of icariin-induced NF-κB activation were investigated in experimental optic nerve ischemia.

Methods

The GOLD bio-informatics tool was used to select target drug based on CEBP-β binding affinity. The neuroprotective effects of target drug, Icariin, were assessed by measuring the flash visual electrode potentials, density of fluorogold-labeled cells, and TUNEL-positive cells in ganglion cell layer. The processes affecting RGC death were probed using optical coherence tomography, immunohistochemistry and immunoblotting techniques.

Results

The simulation analysis and in vivo test demonstrated that the binding complex of icariin and CEBP-β significantly induced endogenous G-CSF expression. A single intravitreal injection of poly(lactic-co-glycolic acid) (PLGA)-icariin preserved visual function and RGC density after optic nerve infarct. The optic nerve edema, RGC apoptosis, and macrophage infiltration were inhibited by treatment with PLGA-icariin. The endogenous G-CSF expression switched the canonical NF-kB activation to the noncanonical NF-kB activation by promoting an alternative phosphorylation reaction of IKK-β. The noncanonical NF-κB activation further promoted the M2 microglia/macrophage polarization and AKT1 activation, which prevented the neuroinflammation and RGC apoptosis Granulocyte colony-stimulating factor.

Conclusion

Our study concluded that the protective mechanism of icariin is a G-CSF-induced non-canonical NF-kB activation, which may provide a potential therapeutic strategy for a patient with neuroinflammation diseases.

Background

Nonarteritic anterior ischemic optic neuropathy (NAION) causes a sudden, acute, and irreversible loss of vision resulting from restricted blood flow in the anterior portion of the optic nerve (ON), which leads to swelling and atrophy of the optic disc [1]. This progresses to acute inflammation and edema, with the ultimate death of the retinal ganglion cells (RGCs) and loss of vision [2]. Macrophage infiltration and the breakdown of the blood–optic nerve barrier (BONB) are crucial events that contribute to inflammation

after ON infarct [3]. Macrophage infiltration typically occurs within 3 days after ON infarct and resolves in about 14 days along with ON edema, contributing to the acute inflammation [2]. This acute neuroinflammatory response catapults the disease progression leading to the loss of the RGCs. A long-lasting anti-inflammatory strategy would be beneficial for countering acute inflammation and prolonged progression of the disease. The increasing incidence of neuroinflammatory diseases has resulted in an urgent need for research on efficient anti-inflammatory therapeutic strategies and drugs that promote neuroprotection.

NF-κB (p65) is an important transcriptional factor that regulates interleukin (IL)−1β as well as many inflammatory cytokines [4]. Its upregulation is associated with the progression of many inflammatory diseases [5]. In an optic nerve injury model, the NF-κB was activated after optic nerve transection, which may mediate RGC apoptosis[6]. Besides, the activation of NF-κB in the astroglia was reported in the model of optic neuritis[7]. It has been suggested that NF-κB activation may be a key pathological factor involved in neuroinflammatory processes secondary to RGC damage. The NF-κB pathway assumes canonical activation in response to lipopolysaccharide or ischemic insult or any other insult, promoting inflammation or noncanonical activation, which is anti-inflammatory [8]. The canonical NF-κB pathway depends on the IKK-β phosphorylation of p65 followed by its nuclear translocation, whereas the noncanonical NF-κB pathway is driven by the IKK-α phosphorylation of p52 followed by its nuclear translocation. The noncanonical NF-κB pathway mediates the regulation of immunity and the anti-inflammatory response [9].

To address NAION, therapeutic strategies have focused on the regulation of neuroinflammation, which includes the inhibition of macrophage infiltration, manipulation of macrophage/microglia polarization, and reduction in the expression of proinflammatory cytokines [10]. Icariin is a flavonoid in traditional Chinese medicine that is generally used for the treatment of erectile dysfunction[11]. It is studied for the treatment of numerous neurodegenerative diseases owing to its anti-inflammatory potential exerted by targeting the Nf-κB signaling pathway [12, 13]. The regulation of Nf-κB activation by icariin remains little known in neuroinflammatory disorders. Icariin has a half-life of 0.16 ± 0.05 h in rat serum [14, 15]. The encapsulation of icariin in poly(lactic-co-glycolic acid) (PLGA) allows for its slow release, thereby increasing its half-life to provide its therapeutic benefits throughout the slow, prolonged, and progressive rAION [16]. The previous report demonstrated that transgenic inhibition of astroglial NF-κB protects from optic nerve damage and retinal ganglion cell loss in experimental optic neuritis[7]. It indicated that long-term inhibition of NF-κB provides a beneficial outcome for optic neuritis treatment.

We hypothesize that a single intravitreal injection of PLGA-icariin could regulate NF-κB activation to provide neuroprotective effects in the experimental optic nerve ischemia. To support this hypothesis, we report the findings of optical coherence tomography (OCT) imaging, retrograde fluorogold labeling, and TUNEL assay, all of which demonstrate that the pathophysiological symptoms of rAION were reduced after treatment with PLGA-icariin. Functionally, the measurements of the amplitude of the flash visual evoked potential (fVEP) indicate restoration of vision after PLGA-icariin treatment. The mechanism of icariin-induced NF-κB activation was further investigated by using simulation analysis, kinase assay, and

immunoblotting assay. Herein, the neuroprotective effects of icariin were reported for the first time in the experimental optic nerve ischemia. The binding complex of icariin and C/EBP-β induced the expression level of endogenous G-CSF to activate the noncanonical NF-κB signaling pathway. We also provided the first evidence for the switch of canonical to noncanonical NF-κB activation via manipulation of phosphorylation target of IKK-β. This G-CSF-induced noncanonical NF-κB activation further improved M2 macrophage/microglia polarization and AKT1 activation, which led to anti-inflammation and anti-apoptosis after optic nerve infarct.

Methods

Study design:

Initially ,rats were separated in three groups *viz* sham ,PBS treated, PLGA-icariin treated. Study began by performing rAION induction on rats from PBS treated and PLGA-icariin treated groups. These groups were monitored and accessed for disease progression and recovery using OCT, fVEP measurements and retrograde fluorogold labeling of RGCs over the period of 28 days. After which the animals were euthanized and the eye samples were processed for histological analysis. The rats for immunoblot analysis were euthanized 3 days post induction. In later development of the study, rats were separated in the three groups *viz* sham, PBS treated and PEG-G-CSF treated. rAION induction was performed in these groups and were euthanized 3 days post induction, their eye samples were processed for immunoblot analysis.

Animals

A total of 36 outbred adult male Wistar rats weighing 150–180 g (7–8 weeks old) were utilized for this study. The rats were obtained from a breeding colony (BioLASCO Co., Yilang, Taiwan). They were maintained in filter-top holding cages and fed *ad libitum* in controlled environmental conditions (temperature 23°C and 55% humidity) with a 12-h light–dark cycle. Animal care and experimental procedures were performed in accordance with the ARVO Statement for the Use of Animals in Ophthalmic and Vision Research. In addition, the Institutional Animal Care and Use Committee at Tzu Chi Medical Center approved all animal experiments. All animal procedures were performed on rats anesthetized by intramuscular injection of ketamine (100 mg/kg) and xylazine (10 mg/kg) cocktail. In all experiments, we utilized Alcaine eye drops (Alcon, Puurs, Belgium) for local anesthesia, Mydrin-P (Santen Pharmaceutical, Osaka, Japan) for pupil dilation, and Tobradex (Alcon, Puurs, Belgium) for wound healing.

rAION induction

After anesthesia, Alcaine and Mydrin-P were applied to the eyes of the rats. Using a 30-gage needle, 2.5 mM of Rose Bengal (RB) in PBS (1 mL/kg animal weight) was injected intravenously through the tail vein. Immediately after the administration of RB to the rats in the PBS-treated group, the right optic disk was exposed to an argon green laser, with a wavelength of 532 nm, size of 500 mm, and power of 80 mW (MC-500 Multicolor Laser, Nidek Co., LTD, Tokyo, Japan). The rats received 12 pulses, each with a 1-s

duration [17]. A brilliant golden glow at the ONH after RB activation by the argon laser was considered as evidence of the successful rAION induction. For the rats in the sham group, the right optic disk was exposed to the argon laser without intravenous injection of RB. Tobradex ointment was applied, after which the rats were kept on a heating pad at 37°C until recovery.

PLGA-icariin administration

Encapsulated PLGA-icariin was obtained from the Industrial Technology Research Institute. PLGA-icariin was prepared by dissolving PLGA-icariin powder (217 ug/mg) in water for injection to a final concentration of 150 μM. PLGA-icariin was administered *via* a single-dose intravitreal injection shortly after rAION induction. Icariin cannot pass the blood-retina-barrier **(Figure S3)** and hence the intravitreal injection confines its therapeutic benefits to the eye system also ensuring no systemic side-effects. The rats in the PBS-treated group received a PBS injection as control, whereas the other 12 rats were given a sham operation and served as the normal group.

Optical coherence tomography

We obtained OCT measurements to measure the opening of Bruch's membrane, as it corresponds to the width of the ONH. We used a Phoenix Micron IV microscope, along with image-guided OCT, with a longitudinal resolution of 1.8 μm and a transverse resolution of 3 μm with a 3.2-mm field of view and 1.2-mm imaging depth at the retina. After anesthesia, the rats were placed at an angle to the lens. Bruch's membrane opening width (ONW) was obtained *via* linear scanning around the optic disk. Images of the ONW were measured using the built-in software Insight (Phoenix Research Labs, CA, USA). This software measures the width of the opening of Bruch's membrane on the micron scale. OCT imaging was conducted for all groups on days 1, 2, 3, 7, 14, 21, and 28.

Retrograde labeling of RGCs by fluorogold

We performed fluorogold retrograde labeling of the RGC 1 week before the animals were sacrificed. The rats were anesthetized, and the skin over the skull was opened. Using the stereotaxic apparatus (Stoelting, Wood Dale, IL, USA), sagittal coordinates were perforated (anterior–posterior [AP]: —6 mm, medial–lateral [ML]: —1.5 mm, dorsal–ventral [DV]: 4 mm) using a motorized dental drill. Using a Hamilton syringe, 2 μL of 5% fluorogold was injected in the superior colliculus (DV, 4 mm). The same procedure was repeated in the other hemisphere [17].

Flash visual evoked potential

At 28 days after rAION induction, fVEP was measured by opening the skin over the skull to expose the sagittal coordinates and implanting three electrodes at the primary visual cortex region of both hemispheres using stereotaxic coordinates (AP, ML, and DV; AP: −8 mm, ML: −3.0 mm). We fixed one electrode at the frontal cortex (AP: 3 mm) and measured the fVEP using the software built into the electrodiagnostic system (Insight, Phoenix Research Labs). The electrode at the primary visual cortex was considered as the active (positive) electrode, the electrode at the frontal cortex was considered as the reference (negative) electrode, and the ground electrode was connected to the rat tail. We measured the

fVEPs using no background Illumination, a flash intensity of 30 cd.s/m^2, and a single flash with a flash rate of 1.02 Hz. We plotted the average of 64 sweeps on a graph. The fVEP measurements were used to calculate the amplitude from the crest of the first positive wavelet (P1) to the trough of the second negative wavelet (N2) [17].

Sample preparation for immunohistochemistry and TUNEL assay

Four weeks after infarct, the rats were euthanized, and their eyes were collected. The eyes were detached along with the ON and transferred to 4% paraformaldehyde to fix the protein sample for 1 day. The samples were then transferred into 30% sucrose and stored at —40°C until they settled to the bottom of the tube as a result of dehydration. The samples were then embedded in OCT molds and stored at —20°C before sectioning. When sectioning, the samples were placed in a cryostat chamber maintained at —20°C, and 30-µm-thick sections of the retina and ON were obtained. We obtained three samples on each slide.

Immunohistochemistry:

The residual OCT compound was washed off by dipping the microscopic slides in PBS for 5 min. The boundary was traced along the sample edge using a liquid blocker to retain the reagents used during the procedure. The tissues were then blocked with 3% bovine serum albumin (BSA) in PBST at room temperature for 1 h. Then, we prepared the primary antibody in 1:100 concentrations in 3% PBST. The tissue samples were then incubated with primary antibody overnight and were subsequently washed with 1X PBS three times for 5 min each. The corresponding secondary antibody was then prepared as a 1:500 concentration in 3% PBST. The tissue samples were incubated with the secondary antibody for 1 h at 37°C in a humid chamber. Then, the samples were washed three times with 1X PBS for 5 min each. Next, the tissue samples were counterstained with DAPI along with the mounting solution using Fluoroshield™ with DAPI. The slides were stored at 4°C until image acquisition using the corresponding filters in the fluorescent microscope. The slides were kept moist throughout the procedure using wet tissue papers.

TUNEL assay

We performed a TUNEL assay to determine whether PLGA-icariin had the potential to rescue the RGCs from apoptosis. The retinal cross-sections containing microscope slides were washed three times with 1X PBS for 5 min each. The borders were then marked along the edge of the sample using a liquid blocker to restrain the reagents used during the procedure. We treated 100 µL of Proteinase K solution (20 ug/mL) on the retina cross-sections for 45 min. The samples were then incubated with 100 µL of kit-provided equilibrium buffer for 10 min at room temperature. Then, 50 µL of TdT reaction mix was prepared per the Promega, DeadEnd™ Fluorometric TUNEL System Kit. The samples were incubated with this TdT reaction mix for 1 h at 37°C in a humid chamber. Humidity was maintained by adding wet tissue papers to the chamber. The samples were then washed with PBS three times for 5 min each, followed by counterstaining with DAPI and sample mounting using Fluoroshield with DAPI. The samples were then kept at 4°C until data acquisition. To collect the data from the samples, we used a confocal microscope

with the corresponding filters. We manually counted the signal from the TUNEL-positive cells in the RGC layer by randomly selecting 10 high-power fields (400×) and calculating the average.

Sample collection for Immunoblotting

The samples were collected at day 3 after infarct after post-euthanasia. The eyeballs with attached ON were surgically scoped out of the rat body. The entire ON was then severed and transferred into an Eppendorf tube at —80°C. The whole-cell protein sample was isolated using RIPA buffer, whereas the cytoplasmic and nuclear protein was isolated using the Biovision Nuclear/Cytosol Fractionation Kit following the standard protocol.

Western blot

Proteins were run on 4–10% precast gradient gel obtained from Invitrogen (Carlsbad, CA, USA) in 1X NuPAGE MOPS running buffer. The 10–20 µg protein sample was loaded in triplicate along with 5 µL of BL Ultra prestained ladder (GeneTex). The proteins were then transferred from the gel onto a PVDF membrane using the iBlot2 system of dry transfer. For this, we used the pre-prepared transfer apparatus from Invitrogen. The membranes were then blocked in 5% nonfat milk in 1X TBST. The primary antibodies were prepared in 5% BSA in 1X TBST. The membrane was incubated in this ECL complex (Immobilon Western Chemiluminescent HRP substrate) complex for 3 min and then mounted on the stage of the iBright fl1000 Imaging system. The results were obtained and quantified using the iBright Analysis software (Invitrogen).

Kinase assay

The Promega Kinase Assay Kit was used along with PTEN pure protein. The IKK-β from the kit was incubated with PTEN pure protein following the kit's protocol. The IKKtide from the kit was incubated with IKK-β, which served as the positive control. Conversely, IKK-β was incubated with the diluent containing adenosine triphosphate alone as a negative control. These three reactions were carried out in individual wells of a 96-well plate.

The reactions were incubated for 30 min, and the luminescence was recorded using iBright FL1000.

insilico **Docking analysis**

GOLD (Genetic Optimization of Ligand Docking) a genetic algorithm (GA) based software, mainly utilizes an evolutionary strategy involving 3 genetic operators; cross overs, mutations and migrations. GOLD imports the partial flexibility to proteins and full flexibility to inhibitors. The Icariin molecule is docked into the active site of CEBP-β from *Homo sapiens* and the interaction of Icariin with the active site residues are thoroughly studied using calculations of molecular mechanics. The parameters used for GA were population size (100), selection pressure (1.1), number of operations (10,000), number of island (1) and niche size. Operator parameters for crossover, mutation and migration were set to 100, 100 and 10 respectively. Default cut off values are, 3.0Å (dH-X) for hydrogen bonds and 6.0Å for van der Waals were employed. The default algorithm speed was selected and the inhibitor binding sites in CEBP-β were

defined within a 10Å radius with the centroid. The number of poses for Icariin was set to 100 and early termination was allowed if the top three bound conformations of inhibitor were within 1.5ÅRMSD. After docking, the individual binding poses of Icariin was observed and the interaction with the CEBP-β was studied. The best and most energetically favorable conformation of Icariin was selected.

GOLD Score fitness function

The four components viz, Protein-ligand hydrogen bond energy (external H-bond); Protein-ligand van der Waals energy (external vdw); Ligand internal van der Waals energy (internal vdw); and Ligand intramolecular hydrogen bond energy (internal- H- bond) were considered for calculating the fitness function of GOLD score. The protein-ligand hydrophobic contact was encouraged by making an empirical correction by multiplying external vdw score with 1.375. The fitness function has been optimized for the prediction of ligand binding positions.

Gold Score = S (hb_ext) + S (vdw_ext) + S (hb_int) + S (vdw_int)

Where,

S (hb_ext) was the protein-ligand hydrogen bond score,

S (vdw_ext) was the protein-ligand van der Waals score,

S (hb_int) was the score from intra molecular hydrogen bond in the ligand

S (vdw_int) was the score from intra molecular strain in the ligand.

Statistical analysis

All statistical analyses were conducted using the GraphPad Prism software. Data are expressed as means ± standard deviations. A nonparametric *t*-test (Mann–Whitney *U* test) was employed for between-group comparisons. A *p*-value of less than 0.05 was considered statistically significant.

Results

PLGA-icariin preserved visual function by inhibiting the RGC apoptosis

In the event of rAION, visual circuitry is disturbed because of axonal damage and loss of the RGCs. The (P1-N2) amplitude was calculated to be 49.24 ± 8.78, 17.21 ± 6.24, and 39.78 ± 14.23 μV in the sham, phosphate-buffered saline (PBS)-treated, and PLGA-icariin groups, respectively. A significant 2.3-fold increase in the amplitude of the PLGA-icariin-treated group was observed compared with the PBS-treated group at day 21($p = 0.0043$). This essentially translates to the significantly preserved visual circuit in the PLGA-icariin-treated group compared with the PBS-treated group (Fig. 1a).

We measured the density of the RGCs on day 28 after rAION induction on a retinal flat were 1841.667 ± 211.68, 502 ± 432.03, and 1780.43 ± 148.6 cells/mm^2, respectively. The RGC density at the central retina in the PBS-treated group exhibited a significant loss in the RGC population (3.5-fold) compared with the sham group, whereas the RGC density in the PLGA-icariin-treated group was significantly increased (2.17-fold) compared with the PBS-treated group (p = 0.0095,p = 0.0061;Figure 1b). This suggests the potential of PLGA-icariin to rescue damaged RGCs.

To support the above findings, we compared the number of apoptotic RGCs in the RGC layer between the groups using a TUNEL assay on the retinal cryosections. The average numbers of TUNEL-positive cells in the RGC layer in the sham, PBS-treated, and PLGA-icariin-treated groups were 0.38, 9.21, and 2.05 cells, respectively (Fig. 1c). TUNEL-positive cells were significantly increased in the PBS-treated group (23.69-fold) compared with the sham group and were significantly reduced in the PLGA-icariin-treated group (4.47-fold) compared with the PBS-treated group(p = < 0.0001,p = 0.0006).

Attenuation of ON edema and macrophage infiltration after PLGA-icariin treatment.

On assessing the damage incurred after rAION *via* OCT, we found that ONH edema was evident since day 1. At this point in time, the opening of Bruch's membrane was the widest in the PBS-treated group, and it gradually decreased with the progression of the disease, resolving after about 7 days. Contrarily, a significant reduction in edema was observed at the ONH in the PLGA-icariin-treated group on day 1 (with an approximate average of 224.5 μm) compared with the PBS-treated group (with an approximate average of 282.6 μm) on day 1 after infarct ($p = 0.018$), whereas the sham group served as a baseline (with an approximate average of 185 μm) (Fig. 2a). The measurements of ON edema were not significantly different in all groups at 7 days after rAION induction.

The high severity of ON edema earlier in the disease progression suggests that the maximum damage is incurred earlier in the timeline. It was found that ON edema can resolve as early as 1 day after PLGA-icariin treatment as evidence of its therapeutic potential.

After immunostaining for the ED1 marker in all groups, the number of ED1-positive macrophages was found to be 1.2 ± 0.7, 12.5 ± 3.4, and 2.28 ± 1.9 in the sham, PBS-treated, and PLGA-icariin-treated groups, respectively. We observed an increased infiltration of macrophages in the PBS-treated group (10.4-fold) compared with the sham group 28 days after rAION induction, which was significantly decreased after PLGA-icariin treatment (5.36-fold) compared with the PBS-treated group(p = < 0.0001,p = 0.0002; Fig. 2b).

Treatment with PLGA-icariin stimulates G-CSF production.

We investigated the potential interaction between CEBP-β and icariin using the GOLD bioinformatics software. Structures prepared by obtained the crystal structure from protein data bank (CEBP-β: 1GTW). For molecular docking, active site of these enzymes was predicted using Castp server. Icariin compound constructed and optimized in Chemsketch software. The statins occupied in the binding sites of CEBP-β were eliminated. The chain A of CEBP-β opted and hydrogen atoms were incorporated into the enzymes

for molecular docking studies.Docking of Icariin into CEBP-β active site was performed and the docking evaluations considered based on GoldScore fitness functions. From the molecular docking of Icariin into active site of CEBP-β, hydrogen bond observed between the hydrogen atom (H4) of Icariin and oxygen atom of ASN281 in CEBP-β with docking score of 42.77. Icariin was found to interact with CEBP-β by binding to its leucine zipper at the C terminal (Fig. 3a,b).

Immunoblot analysis of the retina sample against the G-CSF antibody revealed that G-CSF production was decreased by 1.6-fold after rAION induction whereas treatment with PLGA-icariin was able to increase the G-CSF production by 3.07-fold (p = 0.0286, p = 0.0286; Fig. 3c). In addition, after immunostaining the retinal cross-section, the expression of G-CSF was evident throughout the RGC and RPE layers in the PLGA-icariin-treated group, whereas in the sham and PBS-treated groups, G-CSF was confined to the RGC layer (Fig. 3d).

PLGA-icariin treatment encouraged the propagation of noncanonical NF-κB pathway by promoting a novel IKK-β

Immunoblot analysis of whole-cell protein from ON demonstrated an insignificant change in the NF-κB (p65) levels, with a 1.14-fold increase in the PLGA-icariin-treated group compared with the PBS-treated group(p = 0.4418). However, FAS ligand, which is downstream of the canonical p65 pathway, was found to significantly decrease by 3-fold in the PLGA-icariin-treated group compared with the PBS-treated group(p = 0.0006). The downstream FAS ligand was found to be downregulated contrary to the upregulated NF-κB (p65) (Fig. 4a). To investigate the possibility of noncanonical progression of NF-κB, we measured the cytoplasmic and nuclear protein levels using immunoblot. We found that the ratio of nuclear to cytoplasmic levels of p65 decreased by 2.9-fold in the PLGA-icariin-treated group compared with the PBS-treated group, which confirms that the nuclear localization of NF-κB (p65) was inhibited in the PLGA-icariin-treated group(p = 0.0286).

To access noncanonical activation of NF-κB, we compared the ratio of cytoplasmic and nuclear p52 levels. In the PLGA-treated group, the ratio of p52 levels increased by 2.3-fold compared with the PBS-treated group(p = 0.0022). We also found a significant increase (2.05-fold) on immunoblotting against IKK-α after PLGA-icariin treatment compared to the PBS treated group, suggesting the switch to the noncanonical NF-κB pathway (p = 0.0043;Figure 4b).

The group injected with PEG-G-CSF also demonstrated increased levels of IKK-α (1.48-fold) and p-52 (2.05-fold) compared with the PBS-treated group when their retina was immunoblotted (p = 0.0400, p = 0.0022; Fig. 4c).

Promotion of RGC Survival via **the activation of the PI3K/AKT1 pathway aided by simultaneous**

Immunoblotting demonstrated significantly increased levels of p-PI3K (2.32-fold) and p-AKT1 (5.84-fold) in the PLGA-icariin-treated groups. However, we did not observe any significant upregulation of p-AKT2 (0.52-fold) protein levels when compared with the PBS-treated group(p = 0.0286,p = 0.0095,p = 0.7053).

Immunoblot analysis against the phosphorylated PTEN (p-PTEN) in the retina sample revealed significantly increased p-PTEN levels (3.3-fold) in the PLGA-icariin-treated group compared with the PBS-treated group (p = 0.0022;Figure 5a). This suggests an increased deactivation of PTEN after treatment with PLGA-icariin.

A kinase assay was performed by incubating recombinant human PTEN along with IKK-β. The IKKtide or dilution buffer incubated along with IKK-β served as the positive and negative controls respectively. A significantly (9.79-fold) high luminance signal was detected from the PTEN-incubated chamber compared with the positive control (p = 0.0079;Figure 5b). This proves that IKK-β is a kinase for PTEN. To further evaluate its kinase activity, we predicted the phosphorylation sites on human PTEN sequence by human IKK-β using Kine Phos 2.0 **(Figure S1).**

Promotion of M2 macrophage polarization after PLGA-icariin administration in rAION

Immunoblot analysis showed 5.31-fold increase in CD206 expression in PLGA-Icariin group, in the whole retina protein sample compared to the PBS-treated grou- (p = 0.0286). The upstream p-JAK-1 was increased 1.35-fold while p-STAT3 showed 9.83-fold increase, in the PLGA-Icariin group compared to the PBS-treated group (p = 0.0047,p = 0.0003;Figure 6a). Analysis of the ON sample revealed that the expressions of p-STAT3 and CD206 were increased by 2.7-fold and 2.5-fold, respectively in the PLGA-icariin-treated group, compared with the PBS-treated group(p = 0.0286;p = 0.0286). These results indicate that PLGA-icariin treatment is capable of inducing STAT-3-mediated M2 macrophage/microglia polarization in the ON, whereas analysis of whole-cell protein from the ON head sample revealed that the inflammatory cytokine IL-1β was significantly decreased 14.28-fold in the PLGA-icariin-treated group compared with the PBS-treated group (p = 0.0159;Figure 6b). This indicates that M2 macrophage polarization was promoted after PLGA-icariin treatment in the ON, providing anti-inflammatory benefits at the site of inflammation.

Discussion

In this study, we demonstrated that treatment with PLGA-icariin preserved the visual function and RGC density by inhibiting RGC apoptosis after ON infarct. In addition, the ON edema and the macrophage infiltration were attenuated by icariin treatment. Moreover, we found that icariin bound the transcriptional factor, CEBP-β, to induce endogenous G-CSF production in the retinal cells. The endogenous G-CSF expression promoted noncanonical NF-κB activation to further activate PI3K/AKT1 survival pathway and M2 macrophage polarization.

The visual function was protected by treatment with PLGA-icariin in the rAION model. This protective effect on visual function indicated that treatment with PLGA-icariin suppressed RGC apoptosis after the ischemic insult, which was supported by the evidence of RGC density and TUNEL assay. Baojun Liu et al., reported that icariin treatment reduced the corticosterone-induced apoptosis in rat hippocampal neurons by p38 MAPK inhibition [18]. One recent study demonstrated that the NF-κB mediated apoptosis in fetal

rat hippocampal neurons was attenuated by treatment with icariin [19]. These evidence supported our hypothesis that intravitreal injection of icariin provides neuroprotective effects in the rAION model. Herein, we provided the first evidence that intravitreal injection of icariin inhibited RGC apoptosis and preserved the visual function. However, the protective mechanisms of icariin need further investigation.

The infarct at the ONH causes a breakdown of the BONB, which facilitates the increase in vascular permeability and causes infiltration of the macrophages at the ONH. This further reduces the oncotic pressure gradient, and the hydrostatic pressure in the capillaries of the ON forces out more water, increasing fluid production in the tissue. Thus, the increase in tissue fluid in the ON results in edema at the ON head[2, 3]. In addition, maximum ON edema was observed on day 1 after infarct, but the resolution of ON edema occurred 1 week after ON infract[20]. This implies that ON edema is primarily related to damage to the RGCs in the acute stage of ON ischemia. Contrarily, after treatment with PLGA-icariin, ON edema was found to be decreased on day 1. Therefore, the early relief of swelling pressure on the axons at the ONH may also have contributed to the RGC survival.

After ON infarct, the infiltration of blood-borne macrophages is the major event of inflammation in the ONH [21]. BONB stabilization reduces the infiltration of macrophages and the degree of inflammation, hence reduce RGC death in rAION [22]. The increased ED1-positive macrophages in the ON of the PBS-treated group caused increased local inflammation, whereas fewer macrophages observed at the ONH in the PLGA-icariin-treated group suggest the stabilization of the BONB and post-treatment reduction in macrophage infiltration. This could have also contributed to the resolution of neuroinflammation in the acute stage. Taken together, we suggested that icariin can reduce the breakdown of BONB to attenuate ON edema and macrophage infiltration after ON infarct.

Driven by a binding simulation, we found that icariin has a good binding affinity with CEBP-β. CEBP-β is a known regulator of the G-CSF promoter and is generally present in the system for G-CSF production [23, 24]. The binding of icariin to the C-terminal of CEBP-β, which is known to regulate DNA binding in CEBP-β [25, 26], could have increased its DNA-binding ability and hence promote the increased production of G-CSF. Moreover, CEBP-β regulated transcription coactivator 2 and 3 (CTRC2/3) inhibit the G-CSF production, whereas their depletion is followed by increased STAT3 and G-CSF production via activating the CEBP-β [27, 28]. Our findings demonstrated that intravitreal injection of PLGA-icariin highly induced G-CSF expression in the ganglion cell layer and the retinal pigmented epithelium layer. In addition, our *in vitro* experiment proved the dose-response relationship between icariin and G-CSF in the human RPE cell line **(Figure S2)**. We suggested that Icariin could block the binding of CTRC2/3 to enhance G-CSF production in the retinal cells. G-CSF is a potent neuroprotective agent through anti-inflammation and anti-apoptosis in the experimental model of optic nerve ischemia[10]. Thus, we considered that icariin may trigger endogenous G-CSF expression to modulate the neuroinflammation after ON infarct.

NAION is an inflammatory disease similar to many other neurodegenerative diseases [29–31]. Hence, we expected increased levels of NF-kB (p65) in PBS treated group but not in PLGA-icariin treated group. but to our surprise, the levels of NF-κB remained high after treatment with PLGA-icariin. To gain resolution on

this situation, we checked the protein levels of FAS ligand in all the groups. FAS ligand is known to upregulate under the canonical NF-κB(p65) condition but downregulates while in the noncanonical progression of NF-κB(p52) [32]. FAS ligand was found to be upregulated in the PBS-treated group while downregulated after PLGA-icariin treatment. This suggested the possibility that although NF-κB (p65) may have been upregulated in the PLGA-icariin-treated group, it may not have translocated to the nucleus for the transcription of its downstream products. These doubts were confirmed by the downregulation of the protein levels of p65 in the nucleus in reference to its levels in the cytoplasm. On accessing the p52 levels in the retina, increased translocation of p52 to the nucleus with respect to the cytoplasm was observed in the PLGA-icariin-treated group compared with the PBS-treated group, which corresponds to noncanonical NF-κB progression in the PLGA-icariin-treated group. The upregulation of the noncanonical NF-κB pathway was further confirmed by the increase in the IKK-α levels observed after PLGA-icariin treatment compared with the PBS-treated group [33]. Hence, we considered that PLGA-icariin treatment could promote a switch from the canonical to noncanonical NF-κB pathway. A similar trend was observed after PEG-G-CSF treatment, in which an increase in IKK-α and p52 levels was noted compared to the PBS treated group. This demonstrates that PLGA-icariin treatment could promote noncanonical NF-κB progression *via* the G-CSF-mediated pathway. The noncanonical NF-κB pathway is antiapoptotic in nature and has been reported to regulate inflammation [33]. It also provides anti-inflammatory benefits, whereas its deregulation could promote inflammation [34]. Although the benefits of noncanonical NF-κB are overwhelming, little is known about the mechanism that regulates its switch [35].

With the aim of investigating the interactions that favor the switch to the noncanonical NF-κB pathway, we observed that the upregulated p65 was unable to translocate to the nucleus after PLGA-icariin treatment, which could be explained by the inability of IKK-β to phosphorylate p65 [36]. We also observed that PTEN is phosphorylated rather than being downregulated. The PI3K/AKT pathway is favored by downregulated PTEN, which otherwise gets phosphorylated by scavenging the phosphates from PI3K and inhibits the phosphorylation of PIP2, hence inhibiting the PI3K/AKT pathway [37]. Therefore, PTEN phosphorylation and PI3K/AKT progression are generally mutually exclusive, indicating that another kinase must have acted on the PTEN instead. A previous study demonstrated the ability of the NF-κB pathway to modulate the PTEN activity *via* the observation of decreased PTEN levels in IKK-β(+,+) cells but not in the IKK-β(-,-) cells [38]. There have also been reports suggesting that the NF-κB pathway has an inhibitory effect on the PTEN in the form of a positive feedback loop [39, 40]. Based on the observations and arguments stated above, we suspected the possibility of IKK-β's alternative role in the phosphorylation of PTEN. On assessing the situation *via* kinase assay, we confirmed that IKK-β has the potential for PTEN phosphorylation. In addition, *in-silico* evidence also indicated the ability of human IKK-β to phosphorylate the human PTEN sequence. This explains the unavailability of IKK-β for p65 phosphorylation as well as the presence of the upregulated p-PTEN in the presence of the upregulated PI3K/AKT pathway. This finding suggests that the phosphorylation target of IKK-β plays a decisive role in the progression of the NF-κB pathway. The phosphorylation of p65 by IKK-β leads to the canonical whereas the phosphorylation of PTEN by IKK-β to the noncanonical progression of NF-κB. There is also a possibility that the phosphorylation of PTEN is not the sole alternative target for IKK-β but is rather an

important target, as the noncanonical NF-κB pathway also requires the upregulated PI3K/AKT pathway for its functioning [41]. NF-κB (p65) progression *via* the canonical pathway increases inflammation in rAION and promotes neurodegeneration. Conversely, its switch to the noncanonical pathway after PLGA-icariin treatment, owing to its anti-inflammatory nature, is desired over the canonical progression [34]. The mechanism of this switch *via* the exhaustion of the availability of IKK-β for phosphorylation of p65 could provide a new approach for targeting inflammation.

RGC survival along with G-CSF upregulation suggested that G-CSF influenced the underlying mechanism. The PI3K/AKT survival pathway mediated by the upregulated G-CSF elucidated the rescue of the RGCs along with upregulated PTEN phosphorylation in the retina. Here we report that the upregulation of the PI3K /AKT survival pathway *via* AKT 1 upregulation is sufficient to bring about considerable RGC survival, whereas AKT2 has no role in this process, which is consistent with the findings of a previous study [24].

Macrophages assume either M1 or M2 polarization and previous studies have proved that IKK-α activation inhibits M1 phenotype of the macrophages[42] whereas inactivation of IKK-α is known to increase inflammation in mice[43], which suggested the noncanonical NF-κB signaling pathway could regulate the macrophage polarization. When analyzed by the C206 marker, increased M2 polarized macrophages were recorded at the ON head after treatment with PLGA-icariin. While increased M2 macrophage polarization was found to be promoted *via* the upregulation of phosphorylated STAT3(p-STAT3) [44, 45]. p-STAT3 upregulation is downstream of JAK activation, which is known to be activated upon G-CSF–G-CSF receptor activation [46]. Owing to their high phagocytic ability and ability to produce type 1 inflammatory cytokines, such as IL-1β and tumor necrosis factor–α, M1-type macrophages are inflammatory in nature [47, 48]. As M2 polarization is anti-inflammatory in nature, its benefits were analyzed at the site of primary inflammation, the ON head [17]. Increased IL-1β after rAION represents an upregulated inflammatory response, whereas decreased IL 1-β expression after treatment with PLGA-icariin indicates its anti-inflammatory effects [10, 49]. We also observed the M2 macrophage/microglia polarization in the retina after PLGA-icariin treatment. As the canonical NF-κB progression drives M1 macrophage polarization [50]; based on our observation, the noncanonical NF-κB progression regulates M2 macrophage/microglia polarization and contributes to the anti-inflammatory phenomenon exerted by M2 polarized macrophages/microglia. The degree to which the progression of NF-κB regulates macrophage polarization requires further study.

Conclusion

Collectively, our results demonstrate the neuroprotective potential of a single dose of PLGA-icariin against rAION. G-CSF stimulation by PLGA-icariin in the eye leads to noncanonical NF-κB progression which may have driven the upregulated M2 macrophage polarization and its anti-inflammatory benefits which extend through the restoration of visual function by relieving the physiological stress on the ON and rescuing the RGCs. The survival of RGCs was also improved by the G-CSF mediated upregulation of PI3K/AKT survival pathway. Besides we report, the potential of IKK-β to phosphorylate PTEN and the ability of icariin to exploit this phenomenon to propagate the G-CSF-mediated switch from canonical to noncanonical NF-κB

pathway (Fig. 7). As the noncanonical NF-κB pathway has numerous potential benefits, icariin should be further studied for its ability to favor the switch between the canonical and noncanonical NF-κB pathway.

Abbreviations

1	RGC	Retinal Ganglion cell
2	PLGA	*Poly(lactic-co-glycolic) acid*
3	NAION	*Nonarteritic anterior ischemic optic neuropathy*
4	rAION	Rat model of *Nonarteritic anterior ischemic optic neuropathy*
5	BONB	Blood-Optic nerve barrier
6	ON	Optic nerve
7	OCT	Optical coherence tomography
8	fVEP	Flash visual evoked potentials
9	ONH	Optic nerve head
10	ONW	Optic nerve width
11	ARVO	Association for Research in Vision and Ophthalmology
12	BSA	Bovine serum albumin
13	DNA	Deoxyribose nucleic acid
14	AP	Anterior/posterior
15	ML	Mediolateral
16	DV	Dorsoventral
17	CEBP	CCAAT-enhancer-binding proteins
18	Nf-κB	Nuclear factor kappa light chain enhancer of activated B cells
19	G-CSF	Granulocyte colony-stimulating factor
20	IKK	IκB kinase
21	PTEN	Phosphatase and tensin homolog
22	STAT	Signal transducer and activator of transcription
23	IL	Interleukin

Declarations

Ethical Approval and Consent to participate

Animal care and experimental procedures were performed in accordance with the Association for Research in Vision and Ophthalmology Statement for the Use of Animals in Ophthalmic and Vision Research, and the Institutional Animal Care and Use Committee (IACUC) at the Tzu Chi Medical Center approved all animal experiments.

Consent for publication

Not applicable.

Availability of supporting data:

The data supporting the finding of this study are available within the article and its Supplementary Information files or available from the corresponding author on reasonable request.

Competing interests:

The authors declare no conflicts of interest.

Funding:

This research was funded by the Buddhist Tzu Chi Medical Foundation under the research grant number "TCRD107-30".

Author Contributions:

R-KT, Y-TW and TD conceptualized and designed the research project .R-KT and Y-TW contributed to all the necessary materials, financial support, and laboratory facilities. TD and Y-TW executed all the experiments while JRD performed the *in-silico* analysis in this study. TD and Y-TW contributed to the discussion and interpretation of the raw data. Y-TW and TD contributed to data evaluation and drafting. All authors read and approved the final manuscript.

Acknowledgments: The authors acknowledge the Institute of Eye Research, Hualien Tzu Chi Hospital for experiment assistance. This research was funded by the Buddhist Tzu Chi Medical Foundation under the research grant number "TCRD107-30".

Authors Information:

Affiliations:

Institute of Eye Research, Hualien Tzu Chi Hospital, Buddhist Tzu Chi Medical Foundation, Hualien, Taiwan.

Tushar Dnyaneshwar Desai, Yao-Tseng Wen and Rong-Kung Tsai

Institute of Medical Sciences, Tzu Chi University, Hualien, Taiwan.

Rong-Kung Tsai

Department of Animal Science, Agriculture Research Organization, Volcani center, Israel.

Jayasimha Rayalu Daddam

Corresponding author:

Correspondence to Rong-Kung Tsai

References

1. Berry, S., et al., *Nonarteritic anterior ischemic optic neuropathy: cause, effect, and management.* Eye Brain, 2017. **9**: p. 23-28.
2. Zhang, C., et al., *Optic nerve infarction and post-ischemic inflammation in the rodent model of anterior ischemic optic neuropathy (rAION).* Brain Res, 2009. **1264**: p. 67-75.
3. Salgado, C., et al., *Cellular inflammation in nonarteritic anterior ischemic optic neuropathy and its primate model.* Arch Ophthalmol, 2011. **129**(12): p. 1583-91.
4. Liu, T., et al., *NF-κB signaling in inflammation.* Signal Transduct Target Ther, 2017. **2**: p. 17023-.
5. Mattson, M.P. and S. Camandola, *NF-kappaB in neuronal plasticity and neurodegenerative disorders.* The Journal of clinical investigation, 2001. **107**(3): p. 247-254.
6. Choi, J.S., K.Y. Sungjoo, and C.K. Joo, *NF-kappa B activation following optic nerve transection.* Korean J Ophthalmol, 1998. **12**(1): p. 19-24.
7. Brambilla, R., et al., *Transgenic inhibition of astroglial NF-κB protects from optic nerve damage and retinal ganglion cell loss in experimental optic neuritis.* Journal of Neuroinflammation, 2012. **9**(1): p. 213.
8. Shih, V.F.-S., et al., *A single NFκB system for both canonical and non-canonical signaling.* Cell research, 2011. **21**(1): p. 86-102.
9. Sun, S.-C., *The non-canonical NF-κB pathway in immunity and inflammation.* Nature reviews. Immunology, 2017. **17**(9): p. 545-558.
10. Wen, Y.T., et al., *Early applications of granulocyte colony-stimulating factor (G-CSF) can stabilize the blood-optic-nerve barrier and ameliorate inflammation in a rat model of anterior ischemic optic neuropathy (rAION).* Dis Model Mech, 2016. **9**(10): p. 1193-1202.
11. Makarova, M.N., et al., *Effect of lipid-based suspension of Epimedium koreanum Nakai extract on sexual behavior in rats.* J Ethnopharmacol, 2007. **114**(3): p. 412-6.
12. Li, H., et al., *Icariin Inhibits Endoplasmic Reticulum Stress-induced Neuronal Apoptosis after Spinal Cord Injury through Modulating the PI3K/AKT Signaling Pathway.* Int J Biol Sci, 2019. **15**(2): p. 277-286.

13. Zhang, B., et al., *Icariin attenuates neuroinflammation and exerts dopamine neuroprotection via an Nrf2-dependent manner.* Journal of Neuroinflammation, 2019. **16**(1): p. 92.
14. Sun, M., et al., *Development and Validation of a HPLC-MS/MS Method for Simultaneous Determination of Twelve Bioactive Compounds in Epimedium: Application to a Pharmacokinetic Study in Rats.* Molecules (Basel, Switzerland), 2018. **23**(6): p. 1322.
15. Shen, P., et al., *Simple and sensitive liquid chromatography–tandem mass spectrometry assay for simultaneous measurement of five Epimedium prenylflavonoids in rat sera.* Journal of Chromatography B, 2009. **877**(1): p. 71-78.
16. Hines, D.J. and D.L. Kaplan, *Poly(lactic-co-glycolic) acid-controlled-release systems: experimental and modeling insights.* Critical reviews in therapeutic drug carrier systems, 2013. **30**(3): p. 257-276.
17. Wen, Y.-T., et al., *Early applications of granulocyte colony-stimulating factor (G-CSF) can stabilize the blood-optic-nerve barrier and ameliorate inflammation in a rat model of anterior ischemic optic neuropathy (rAION).* Disease models & mechanisms, 2016. **9**(10): p. 1193-1202.
18. Liu, B., et al., *Neuroprotective effects of icariin on corticosterone-induced apoptosis in primary cultured rat hippocampal neurons.* Brain Res, 2011. **1375**: p. 59-67.
19. Liu, J., et al., *Icariin Protects Hippocampal Neurons From Endoplasmic Reticulum Stress and NF-κB Mediated Apoptosis in Fetal Rat Hippocampal Neurons and Asthma Rats.* Front Pharmacol, 2019. **10**: p. 1660.
20. Kapupara, K., et al., *Optic nerve head width and retinal nerve fiber layer changes are proper indexes for validating the successful induction of experimental anterior ischemic optic neuropathy.* Exp Eye Res, 2019. **181**: p. 105-111.
21. Chang, C.H., et al., *Neuroprotective effects of recombinant human granulocyte colony-stimulating factor (G-CSF) in a rat model of anterior ischemic optic neuropathy (rAION).* Exp Eye Res, 2014. **118**: p. 109-16.
22. Huang, T.L., et al., *Early Methylprednisolone Treatment Can Stabilize the Blood-Optic Nerve Barrier in a Rat Model of Anterior Ischemic Optic Neuropathy (rAION).* Invest Ophthalmol Vis Sci, 2017. **58**(3): p. 1628-1636.
23. Chang, S.-F., et al., *LPS-Induced G-CSF Expression in Macrophages Is Mediated by ERK2, but Not ERK1.* PLOS ONE, 2015. **10**(6): p. e0129685.
24. Nguyen Ngo Le, M.-A., et al., *Therapeutic Effects of Puerarin Against Anterior Ischemic Optic Neuropathy Through Antiapoptotic and Anti-Inflammatory Actions.* Investigative Ophthalmology & Visual Science, 2019. **60**(10): p. 3481-3491.
25. Lee, S., et al., *RSK-mediated phosphorylation in the C/EBP{beta} leucine zipper regulates DNA binding, dimerization, and growth arrest activity.* Mol Cell Biol, 2010. **30**(11): p. 2621-35.
26. Lekstrom-Himes, J. and K.G. Xanthopoulos, *Biological Role of the CCAAT/Enhancer-binding Protein Family of Transcription Factors *.* Journal of Biological Chemistry, 1998. **273**(44): p. 28545-28548.
27. Kim, J.H., et al., *CREB coactivators CRTC2 and CRTC3 modulate bone marrow hematopoiesis.* Proc Natl Acad Sci U S A, 2017. **114**(44): p. 11739-11744.

28. Kim, J.H., et al., *CREB coactivators CRTC2 and CRTC3 modulate bone marrow hematopoiesis.* Proceedings of the National Academy of Sciences, 2017. **114**: p. 201712616.
29. Amor, S., et al., *Inflammation in neurodegenerative diseases.* Immunology, 2010. **129**(2): p. 154-69.
30. Gorman, A.M., *Neuronal cell death in neurodegenerative diseases: recurring themes around protein handling.* J Cell Mol Med, 2008. **12**(6a): p. 2263-80.
31. Mehrabian, Z., et al., *Oligodendrocyte death, neuroinflammation, and the effects of minocycline in a rodent model of nonarteritic anterior ischemic optic neuropathy (rNAION).* Mol Vis, 2017. **23**: p. 963-976.
32. Liu, F., et al., *NF-κB directly regulates Fas transcription to modulate Fas-mediated apoptosis and tumor suppression.* The Journal of biological chemistry, 2012. **287**(30): p. 25530-25540.
33. Sun, S.C., *The non-canonical NF-κB pathway in immunity and inflammation.* Nat Rev Immunol, 2017. **17**(9): p. 545-558.
34. Sun, S.-C., *Non-canonical NF-κB signaling pathway.* Cell research, 2011. **21**(1): p. 71-85.
35. Israël, A., *The IKK complex, a central regulator of NF-kappaB activation.* Cold Spring Harbor perspectives in biology, 2010. **2**(3): p. a000158-a000158.
36. Kawai, T. and S. Akira, *Signaling to NF-kappaB by Toll-like receptors.* Trends Mol Med, 2007. **13**(11): p. 460-9.
37. Georgescu, M.-M., *PTEN Tumor Suppressor Network in PI3K-Akt Pathway Control.* Genes & cancer, 2010. **1**(12): p. 1170-1177.
38. Vasudevan, K.M., S. Gurumurthy, and V.M. Rangnekar, *Suppression of PTEN expression by NF-kappa B prevents apoptosis.* Mol Cell Biol, 2004. **24**(3): p. 1007-21.
39. Wang, X., et al., *NEDD4-1 is a proto-oncogenic ubiquitin ligase for PTEN.* Cell, 2007. **128**(1): p. 129-139.
40. Carracedo, A. and P.P. Pandolfi, *The PTEN–PI3K pathway: of feedbacks and cross-talks.* Oncogene, 2008. **27**(41): p. 5527-5541.
41. Gustin, J.A., et al., *Akt regulates basal and induced processing of NF-kappaB2 (p100) to p52.* J Biol Chem, 2006. **281**(24): p. 16473-81.
42. Li, T., et al., *MicroRNAs modulate the noncanonical transcription factor NF-kappaB pathway by regulating expression of the kinase IKKalpha during macrophage differentiation.* Nat Immunol, 2010. **11**(9): p. 799-805.
43. Lawrence, T., et al., *IKKalpha limits macrophage NF-kappaB activation and contributes to the resolution of inflammation.* Nature, 2005. **434**(7037): p. 1138-43.
44. Lang, R., et al., *Shaping gene expression in activated and resting primary macrophages by IL-10.* J Immunol, 2002. **169**(5): p. 2253-63.
45. Liu, Y.C., et al., *Macrophage polarization in inflammatory diseases.* Int J Biol Sci, 2014. **10**(5): p. 520-9.

46. Marino, V.J. and L.P. Roguin, *The granulocyte colony stimulating factor (G-CSF) activates Jak/STAT and MAPK pathways in a trophoblastic cell line.* J Cell Biochem, 2008. **103**(5): p. 1512-23.
47. Mosser, D.J.J.o.L.B., *The many faces of macrophage activation.* 2003. **73**.
48. Beyer, M., et al., *High-Resolution Transcriptome of Human Macrophages.* PLOS ONE, 2012. **7**(9): p. e45466.
49. Stojakovic, A., et al., *Role of the IL-1 Pathway in Dopaminergic Neurodegeneration and Decreased Voluntary Movement.* Molecular neurobiology, 2017. **54**(6): p. 4486-4495.
50. Wang, N., H. Liang, and K. Zen, *Molecular mechanisms that influence the macrophage m1-m2 polarization balance.* Front Immunol, 2014. **5**: p. 614.

Figures

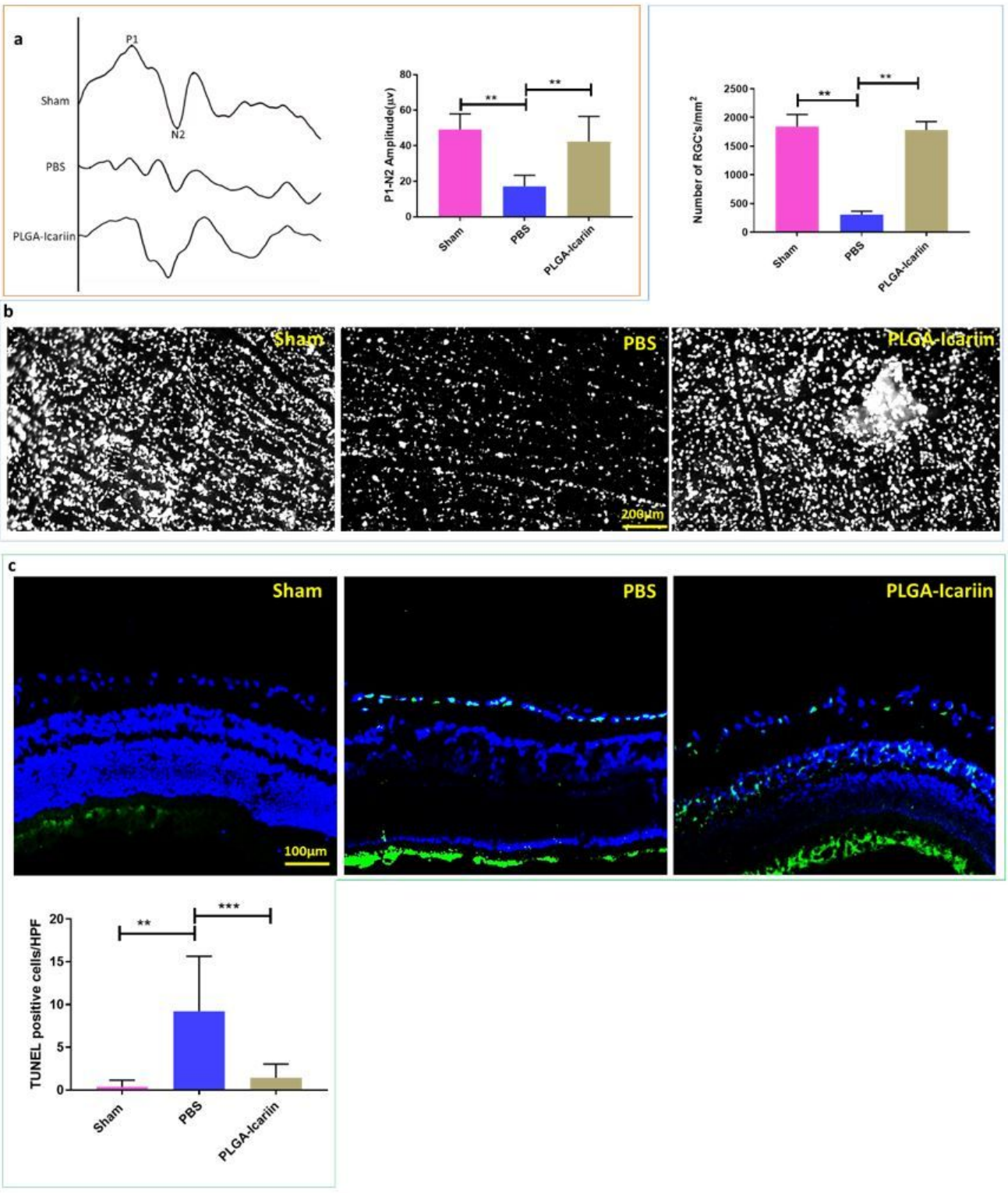

Figure 1

Significant recovery of the functional visual circuitry and rescue of RGCs, 28 days after intravitreal injection of PLGA-icariin, as evidenced by the fVEP measurements, retrograde flurogold labeling and TUNEL assay. a. Representative fVEP signals with labeled P1-N2 amplitude for each group measured 28 days after treatment. b. The P1-N2 amplitude significantly depreciated after the rAION induction recovered after treatment with PLGA-icariin. **P ≤ 0.01, n = 6 in each group. b. The RGCs (white spots) on

the peripheral retina. Graphical representation of the RGC density compared among the different groups. c. TUNEL-positive cells (green) in contrast to the other cells (blue) in the retina. Quantification of the TUNEL-positive cells under high-power field among each group. ***P ≤ 0.001, ****P ≤ 0.0001, n = 6 in each group.

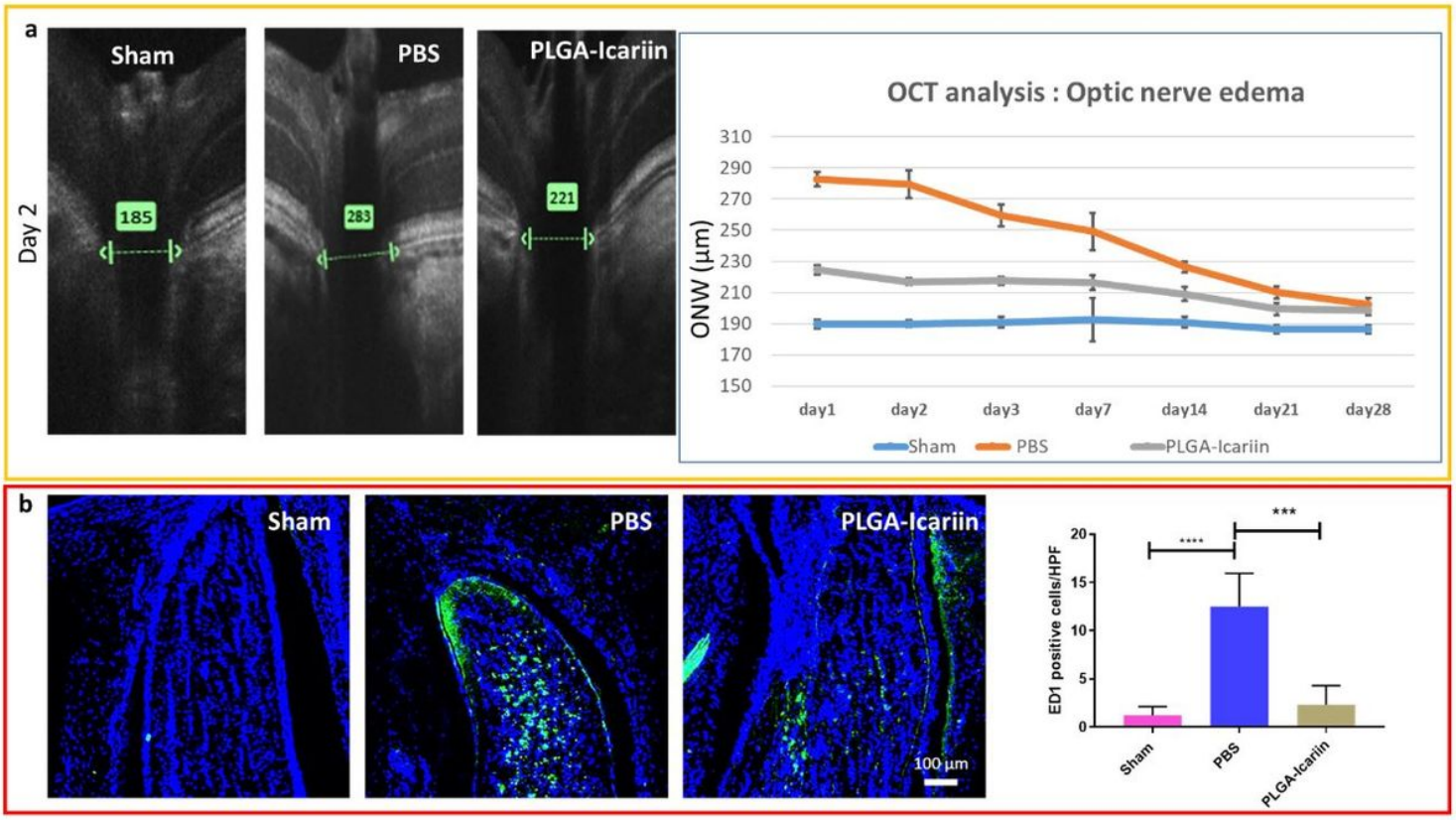

Figure 2

The OCT performed on the ONH reveals that edema of Bruch's membrane resolved earlier in the timeline of the rAION progression along with reduced macrophage infiltration in the ONH. a. Representative OCT image showing the different layers of the retina at the ONH. The green arrow indicates the distance measured between the same retinal layer on either ends of the ONH. Graphical quantification presents the width of the optic nerve over different time points in all groups. b. Immunohistochemistry staining for macrophages bearing the ED1 marker (green) signals in contrast to the DAPI (blue) signals in all groups. The graphical quantification of the macrophage density in different groups. *P ≤ 0.05, ***P ≤ 0.001; n = 6 in each group.

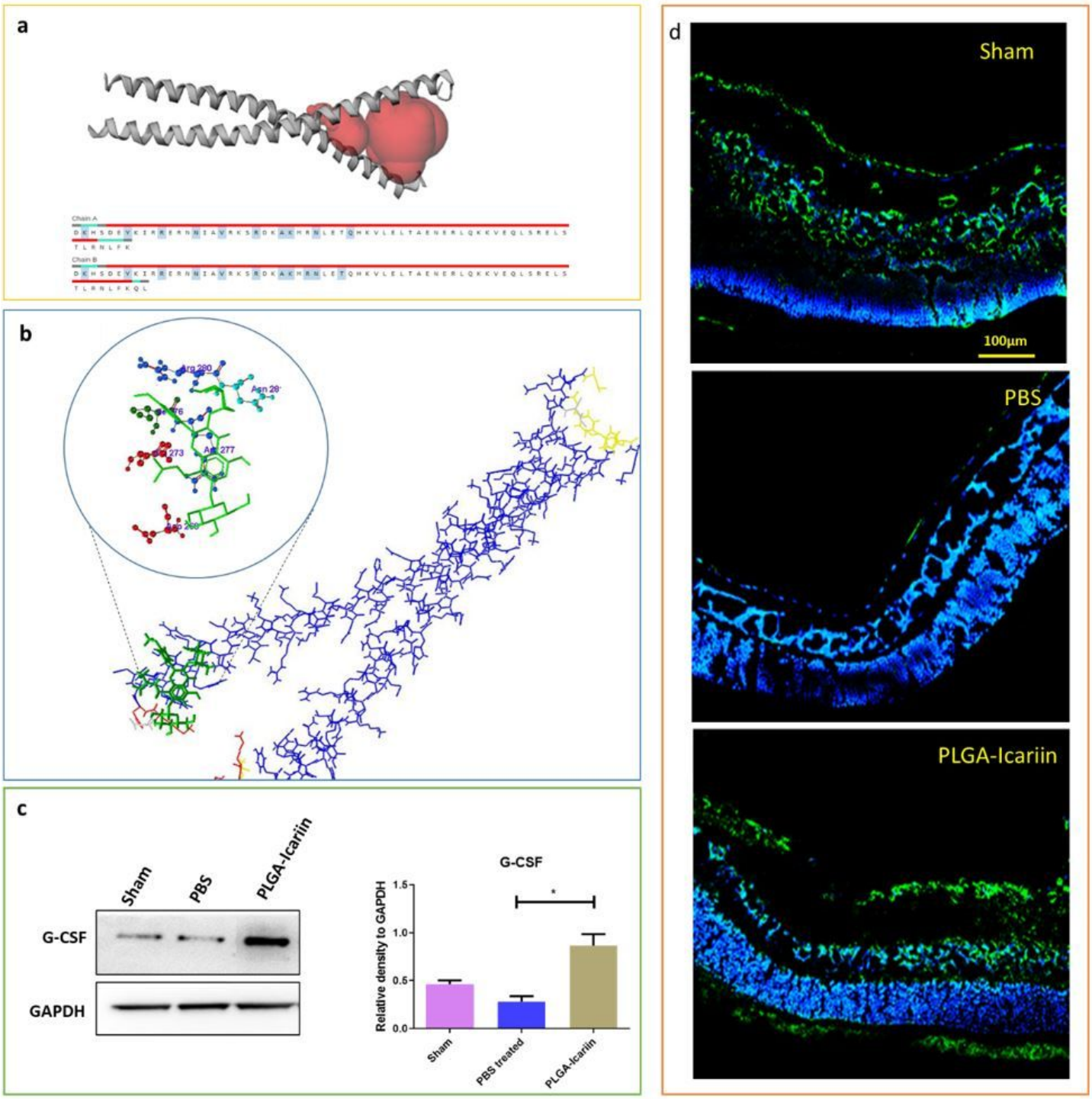

Figure 3

Icariin interacts with CEBP-β to regulate G-CSF production in retinal cells. a. Docking studies using the GOLD software showing the interaction of icariin (green) with CEBP-β (blue). b. Active site of CEBP-β showing the DNA-binding site for CEBP-β. c. Immunoblot analysis for the G-CSF levels in the retina and quantification for the same. d. Immunohistochemistry staining for G-CSF demonstrates its presence in different treatment conditions in the retina. *P ≤ 0.05, n = 3 in each group.

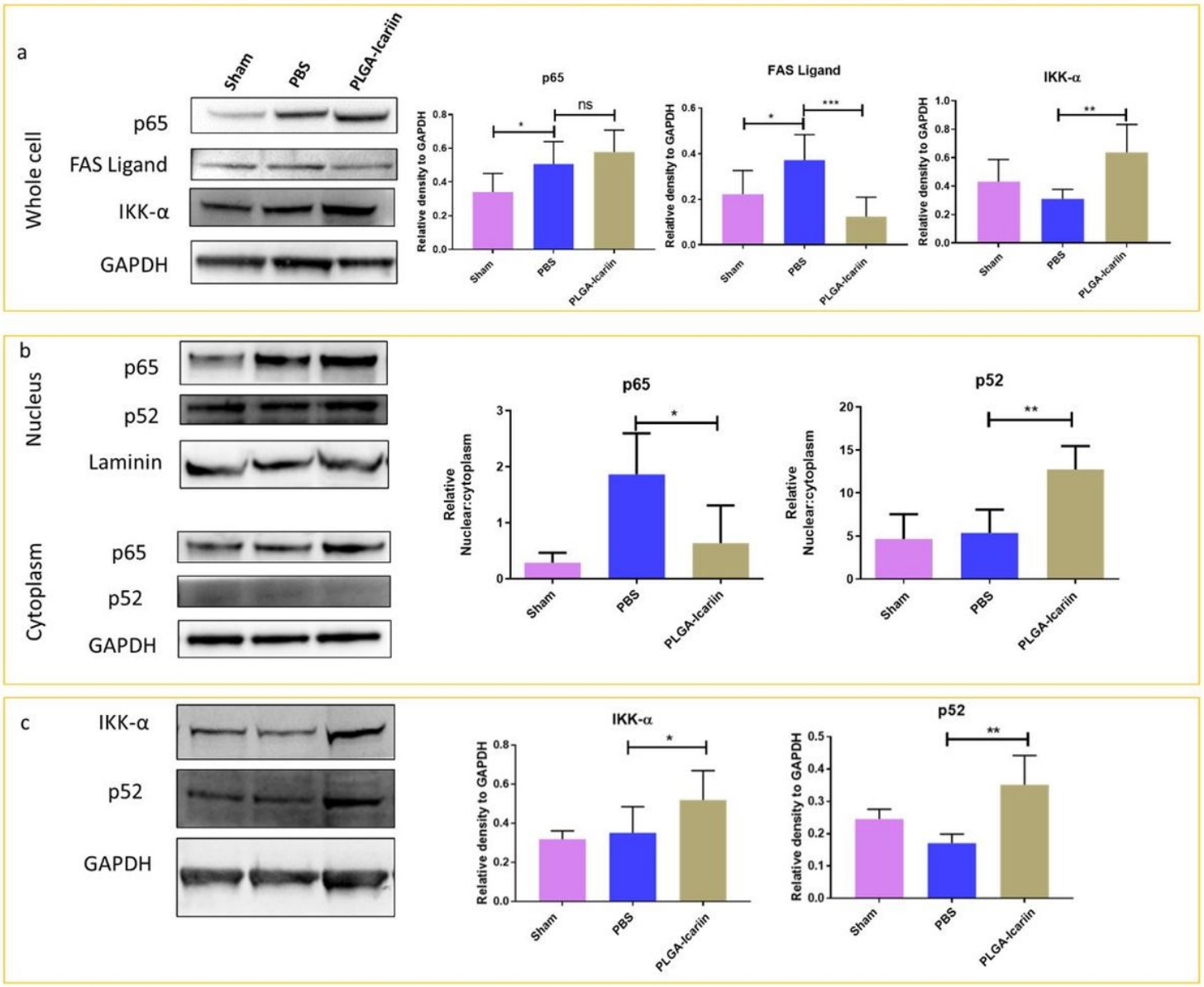

Figure 4

Immunomodulation of NF-κB to its anti-inflammatory noncanonical pathway after PLGA-icariin treatment a. Western blot analysis of p65, FAS ligand, IKK-α, and GAPDH. Quantification of these proteins normalized to GAPDH. b. Immunoblot of p65, p52, and laminin protein levels in the nuclear fraction of the retina. The quantification of these proteins normalized to laminin and Western blot of p65, p52, and GAPDH protein levels in the cytoplasmic fraction of the retina. These protein levels were normalized to GAPDH. c. Western blot analysis of IKK-α and p-52 on the whole retina in the sham, rAION, and PEG-G-CSF groups. ns, $P > 0.05$, *$P \leq 0.05$, **$P \leq 0.01$, ***$P \leq 0.001$, n = 3 in each group.

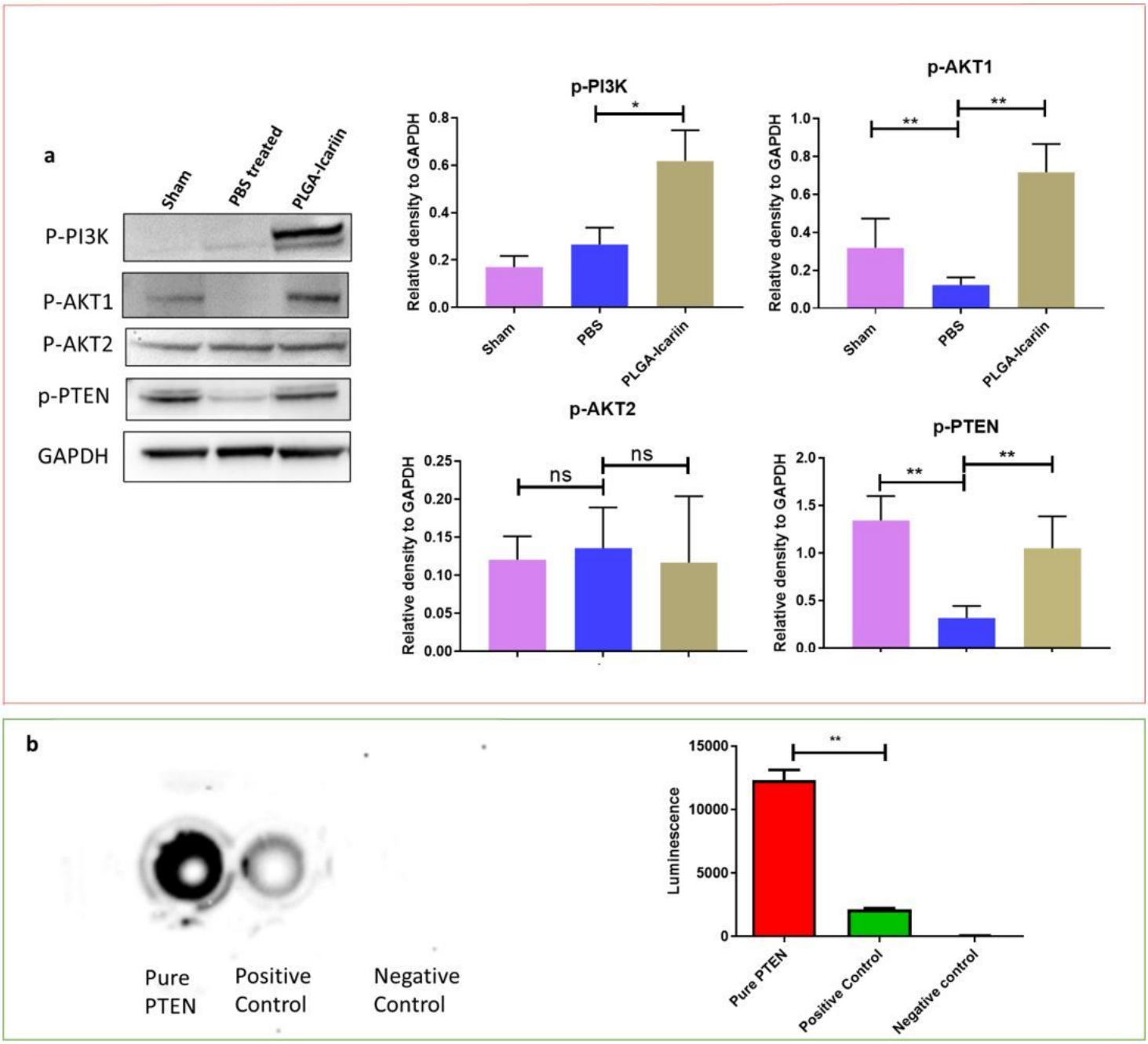

Figure 5

Survival of RGCs mediated by AKT1 and not by AKT2 after PLGA-icariin treatment. Kinase assay for human recombinant IKK-β against PTEN. a. Western blot for the protein levels of p-PI3K, p-AKT1, p-AKT2, p-PTEN, and GAPDH. b. Quantification of the protein levels normalized to GAPDH. *P ≤ 0.05, **P ≤ 0.01, ns P > 0.05; n = 3 in each group. c. The luminescence after IKK-β kinase exposure with pure PTEN, positive control, and negative control. d. Graphical representation of the quantified luminescence signal. **P ≤ 0.01.

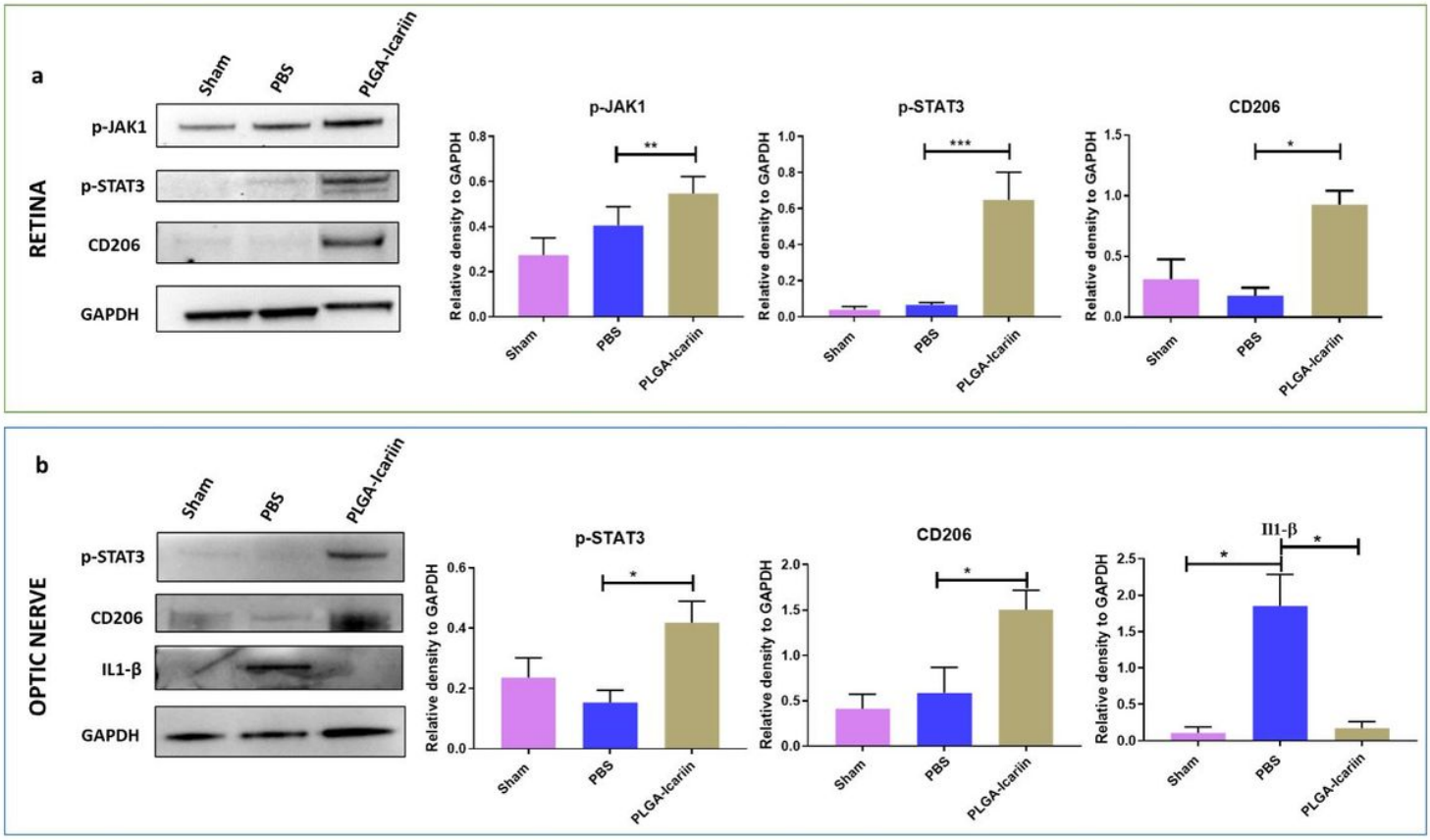

Figure 6

PLGA-icariin promotes STAT-3-mediated M2 macrophage polarization in ON. Western blot analysis of the protein levels of p-STAT3 and CD206 in ON, along with the IL-1β protein levels in the ON. Quantification of the protein levels normalized to GAPDH in the ON depicted in the graphical representation. *P ≤ 0.05, **P ≤ 0.01, ***P ≤ 0.001; n = 3 in each group.

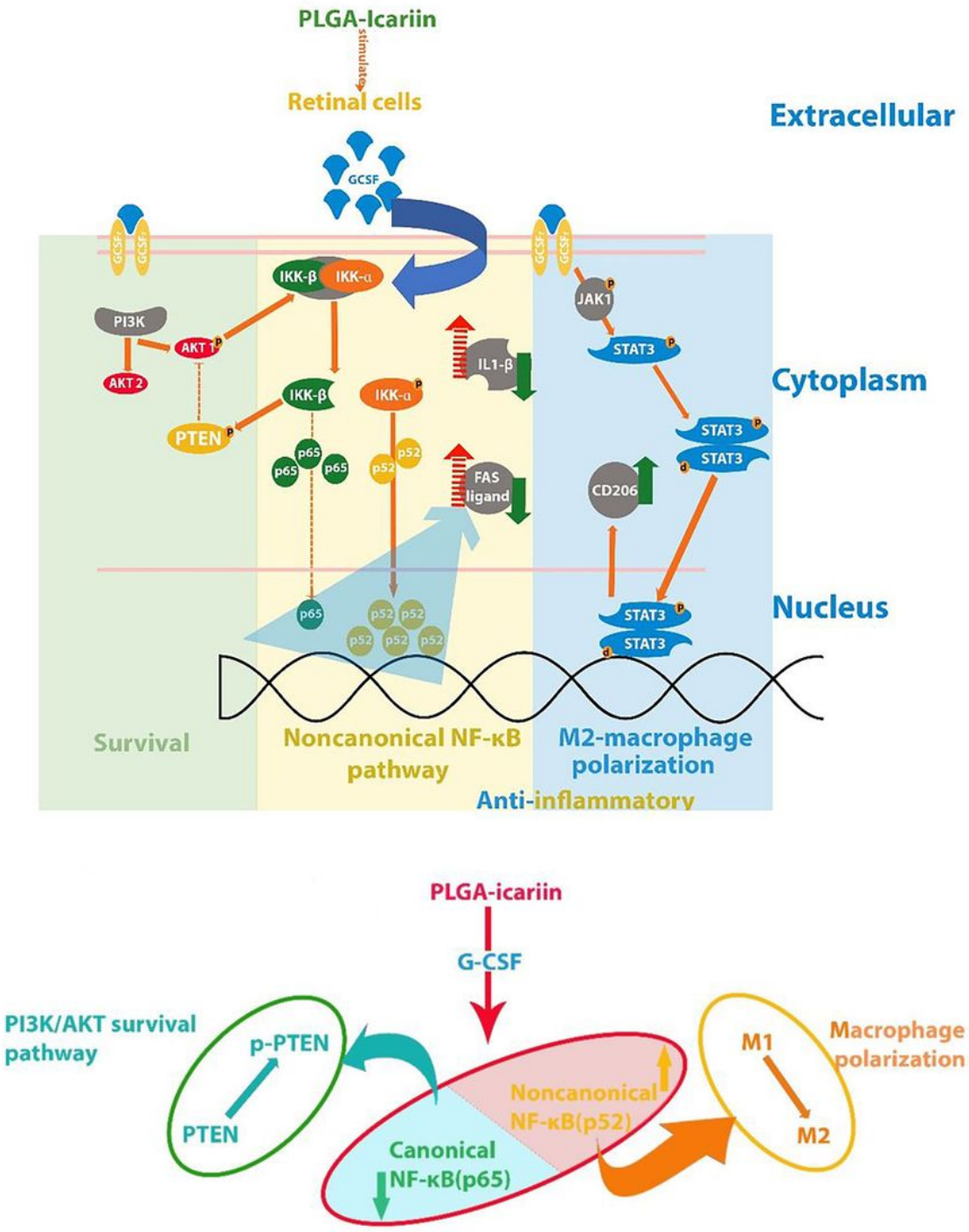

Figure 7

Summary The neuroprotective potential of PLGA-icariin treatment summarized by the survival of RGCs, anti-inflammatory activity, and M2 macrophage polarization along with their interactions.

Supplementary Files

This is a list of supplementary files associated with this preprint. Click to download.

- SupplementaryMaterials.docx